How to Cite:
Vawhal, P. K., & Jadhav, S. B. (2022). Design, synthesis, and biological evaluation of 3-chloro-2-oxo-N-(arylcarbamoyl)-2H-1-benzopyran-6-sulfonamide derivatives as potential DPP-IV inhibitors. *International Journal of Health Sciences, 6*(S3), 373–392. https://doi.org/10.53730/ijhs.v6nS3.5190

Design, Synthesis, and Biological Evaluation of 3-Chloro-2-Oxo-N-(Arylcarbamoyl)-2H-1-Benzopyran-6-Sulfonamide Derivatives as Potential DPP-IV Inhibitors

Pallavi Kishor Vawhal
PEA's Modern college of Pharmacy, Sector 21, Yamunanagar, Nigdi- 411044 India

Shailaja B. Jadhav
PEA's Modern college of Pharmacy, Sector 21, Yamunanagar, Nigdi- 411044 India

***Abstract*---**In present work, we aimed at preparing coumarin and sulfonamide containing moieties into a single candidate template i.e. 3-chloro-2-oxo-N-(arylcarbamoyl)-2H-1-benzopyran-6-sulfonamides for the purpose of synergistic activity as potent DPP-IV inhibitors. The designed derivatives were subjected for the calculations of Lipinski rule, Veber's rule, ADME analysis, drug-likeness properties and molecular docking. The derivatives which successfully passed all the criteria were proceeded for wet lab synthesis and biological evaluation. From the initial screening through Lipinski rule, Veber's rule, ADME calculations, and drug-likeness properties, molecules 1a, 1f, 1g, 1h, 1i, 1j, 1k, 1o, 1p, 1q, 1r, 1v, 1w, and 1x successfully passed all the filters and displayed most drug-likeness nature. Therefore only these molecules were subjected for molecular docking studies. From molecular docking results, we have selected 1f, 1g, 1i, 1j, and 1v for the wet lab synthesis and biological evaluation. The structures of all the synthesized compounds were confirmed by spectral analysis and were subjected for in vitro DPP-IV enzyme assay. Sitagliptin was used as standard for the assay and it displayed 0.018 µM IC50 value. Compound 1f, 1g, 1i, 1j, and 1v exhibited 15.55, 15.85, 13.95, 14.48, and 13.45 µM IC50 values respectively. We concluded that compound 1f, 1g, 1i, 1j, and 1v are potential lead compounds to be developed as potent DPP-IV inhibitors for the treatment of diabetes.

***Keywords*---**DPP-IV inhibitors, coumarin derivatives, molecular docking, ADME, vitro.

International Journal of Health Sciences ISSN 2550-6978 E-ISSN 2550-696X © 2022.
***Corresponding author**: Vawhal, P. K.; Email: vawhalpallavi@gmail.com*
Manuscript submitted: 18 Nov 2021, Manuscript revised: 09 Feb 2022, Accepted for publication: 27 March 2022

Introduction

Chronic diseases such as diabetes mellitus pose a serious hazard to human health across the globe. Diabetes type 2 (T2DM) is characterised by insulin resistance and poor glucose homeostasis, which leads to hyperglycemia(Artasensi et al., 2020). Anti-diabetic medications now on the market include sulfonylureas, meglitinides, thiazolidinediones, biguanides, and alpha-glucosidase inhibitors, all of which attempt to reduce hepatic glucose production, stimulate insulin release, reduce glucose absorption, and increase peripheral glucose utilization(Grewal et al., 2020; Vojislav et al., 2020). Weight gain and hypoglycemia are common adverse effects of these medications, making it difficult to maintain optimal glycemic control for an extended period of time. Many additional techniques to better managing T2DM have thus evolved, each with its own unique mechanism of action(Galicia-Garcia et al., 2020; Kelly and Neary, 2020; Simos et al., 2020). Diabetic patients with type 2 diabetes may benefit from modern treatments such as dipeptidyl peptidase-IV (DPP-IV) inhibitors, which have shown long-term effectiveness and improved glucose control. The regeneration and differentiation of pancreatic beta-cells is aided by DPP-IV inhibitors, which have also been shown to be well tolerated and to reduce hypoglycemia and cardiovascular adverse effects(Dowarah and Singh, 2020; Huang et al., 2019; Okechukwu et al., 2020).

The biliary system, kidney, gastrointestinal tract, uterus, and liver are just some of the places where DPP-IV may be found in the human body. This enzyme is essential for the regulation of incretin hormones, as well as a signaling factor for glucagon-like peptide (GLP-1) and glucose-dependent insulinotropic polypeptide (GIP) (GIP). One of the most important roles of these hormones is to increase insulin production and reduce the death of beta-cells. For both GLP-1 and GIP, the half-life is only 1–2 minutes, and 7 minutes for GIP. This is due to the fast degradation by DPP-IV. Sitagliptin, Alogliptin, Linagliptin, Anagliptin and Teneligliptin are some of the structurally varied DPP-IV inhibitors currently on the market(Arulmozhi and Portha, 2006; Safavi et al., 2013; Salvatore et al., 2007; Stoimenis et al., 2017).

Coumarins are a vital category of common oxygen heterocyclic composites. The coumarins have various biological activities and their therapeutic effects are given significant attention in developing many drugs with high activity(Sashidhara et al., 2014). The solubility and stability of compounds are those properties that give the highest applicability of medicinal purpose compounds to the medical chemist. Coumarin derivatives consist of numerous biological activities, e.g. anticoagulant, anticonvulsant, antihypertensive, anti-inflammatory, anti-adipogenic, neuroprotective, antioxidant, and anti-hyperglycemic traits, in addition to extensive cytotoxic impacts towards bacteria, tubercular cells, cancer cells, fungi, viruses, phytoalexin, hypnotic, anti-helminthic, insecticidal, and HIV protease constraints. The naturally generated coumarins are selectively stereo-specific and construct natural products like alkaloids, macrolides, terpenoids, and pheromones. The widespread use of the coumarin groups includes designing fluorescent chemo sensors, tagging polymers, solar cells, cellular imaging tools, and extensive utilization for the purpose of synthesizing laser dyes(De Souza et

al., 2005; Galayev et al., 2015; Tamene and Endale, 2019; Teoh and Das, 2018). In present work, we aimed at preparing coumarin and sulfonamide containing moieties into a single candidate template i.e. 3-chloro-2-oxo-N-(arylcarbamoyl)-2H-1-benzopyran-6-sulfonamides for the purpose of synergistic activity as potent DPP-IV inhibitors. The designed derivatives were subjected for the calculations of Lipinski rule, Veber's rule, ADME analysis, drug-likeness properties and molecular docking. The derivatives which successfully passed all the criteria were proceeded for wet lab synthesis and biological evaluation.

Material and Methods

Reaction scheme and derivatives

The derivatives were designed by taking 2-hydroxybenzaldehyde as starting material which have to be treated with different organic compounds/reagents to produce 3-chloro-2-oxo-2H-1-benzopyran-6-sulfonamide. It was then treated with diphosgene and substituted anilines to get final derivatives. The proposed reaction scheme is depicted in Fig. 1.

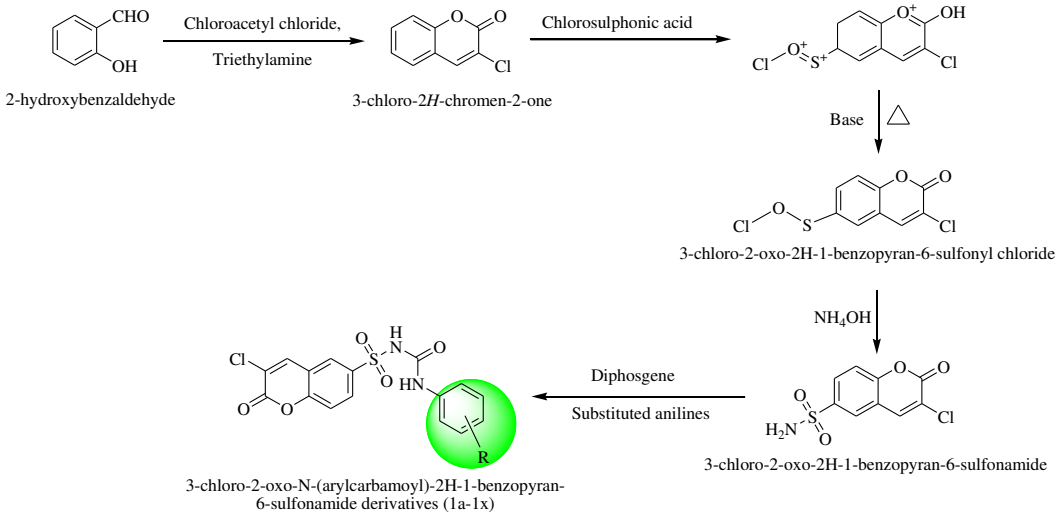

Figure 1. The proposed reaction scheme to design 3-chloro-2-oxo-N-(arylcarbamoyl)-2H-1-benzopyran-6-sulfonamide derivatives

Pharmacokinetics predictions of designed derivatives

The Lipinski rule of five and the pharmacokinetic (ADME) characteristics of designed derivatives were investigated using PubChem(Kim et al., 2021), molinspiration("Molinspiration cheminformatics," 2006), and SwissADME(Daina et al., 2017) servers.

Molecular docking studies

In order to further optimization, the derivatives were subjected for binding affinity studies with DPP-IV enzyme. The Autodock vina 1.1.2 with PyRx Virtual Screening Tool 0.8 software of the Chimera version 1.10.2(Dallakyan and Olson, 2015) and the Biovia Discovery studio was used to perform molecular docking(Miyata, 2015). The structures of 3-chloro-2-oxo-N-(arylcarbamoyl)-2H-1-benzopyran-6-sulfonamide derivatives and native ligand were drawn using ChemDraw Ultra 8.0 version and saved in mol file format. The energy minimization was executed by Universal Force Field (UFF) in PyRx software(Rappé et al., 1992). The crystal structure of the human DPP-IV in complex with a cyclohexalamine inhibitor (PDB ID: 2P8S) was obtained from the RCSB Protein Data Bank (https://www.rcsb.org/). The 3D ribbon view of DPP-IV in complex with native ligand is illustrated in Fig. 2. The binding mode and binding affinity of native ligand was used to validate the results of designed derivatives. With an exhaustiveness value of 8, the three-dimensional grid box (size_x = 62.5455580638A^{o}, size_y = 68.1442437431A^{o}, size_z = 64.3386815524A^{o}) was modified for molecular docking simulations. The complete molecular docking approach was carried out in accordance with the methods outlined by S. L. Khan *et al.*(Chaudhari et al., 2020; Khan, Sharuk L; Siddiui, 2020; S. Khan et al., 2021; Khan et al., 2020; S. L. Khan et al., 2021; Siddiqui et al., 2021).

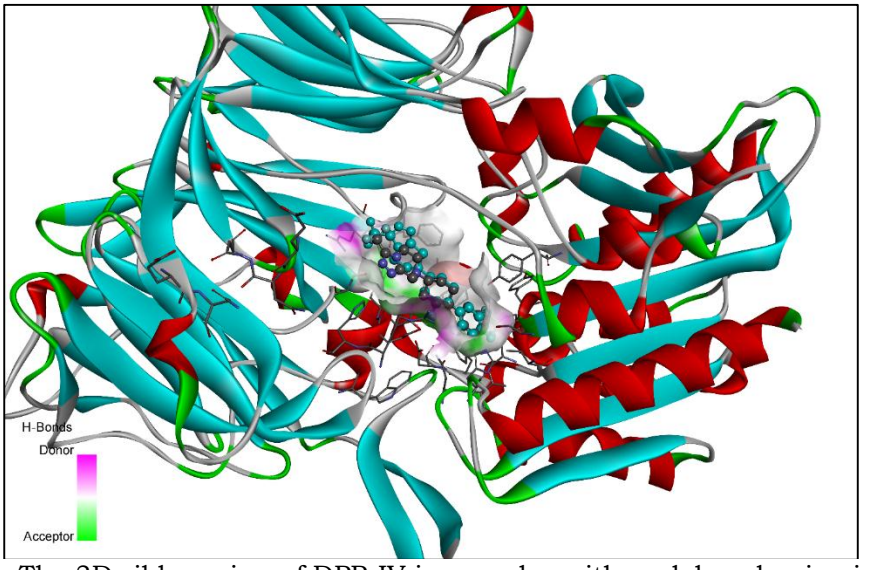

Figure 2. The 3D ribbon view of DPP-IV in complex with cyclohexalamine inhibitor (native ligand)

Wet lab synthesis of selected derivatives

The chemicals of synthetic grades such as 2-hydroxybenzaldehyde, chloroacetyl chloride, dichloromethane, trimethylamine, chlorosulphonic acid, NH_4OH, and substituted anilines were purchased and procured from Lab Trading Chemicals, Auranagabad, Maharashtra, India.

Step-I: Synthesis of 3-chloro-2H-chromen-2-one
Solution of 2-hydroxybenzaldehyde (3.75 mol) in dichloromethane (4 ml) was added in triethylamine (8.6 mol) and a solution of chloroacetyl chloride (5.02 moles) under continuous stirring in cold condition. The above cold solution was added in 2ml methylene chloride. The mixture was stirred at room temperature for 30 min. and then heated to reflux for 8-10 hrs. The solvent was removed under reduced pressure and the dark brown oily residue was chromatographed over silica gel (100-200 mesh) using n-hexane as an eluent to give some amount of starting compound and 3-chlorocoumarin as crystalline products. The yields reported are based on recovered starting compound. All 3-chlorocoumarins were recrystallized from n -hexane(Mali and Deshpande, 1995).

Step-II: Synthesis of 3-chloro-2-oxo-2H-1-benzopyran-6-sulfonyl chloride
Chlorosulfonic acid (4 ml, 0.06 mol) was cooled in ice bath and treated with 4.32-4.40 gm of 3-chlorocoumarin separately (1 mol) at such a rate that the reaction temperature was maintained between 10-15 °C for almost 35 minutes. The ice bath was removed and the solution was stirred at room temperature for 16 hrs. The mixture was diluted with dichloromethane and the solution was slowly added to ice water with stirring. From the two phases which were separated, the dichloromethane portion was collected and cooled to 5 °C and then treated with conc. NH_4OH and stirred at 15 °C for 15 min. The mixture was then extracted with dichloromethane, filtered and concentrated to give crude products. The crude products were dissolved to 2-butanone and then recrystallized using isopropyl alcohol(Basanagouda et al., 2010).

Step-III: Synthesis of 3-chloro-2-oxo-2H-1-benzopyran-6-sulfonamide
The prepared 3-chloro-2-oxo-2H-1-benzopyran-6-sulfonyl chloride (0.5 mol) was boiled for ten minutes with concentrated ammonium hydroxide (5cc). After cooling to room temperature, and adding cold water (10cc), the resultant solid sulphonamide was filtered with suction and thoroughly washed. It was then recrystallized to constant melting point from dilute ethanol and dried at 105 ^oC(Qi and Zhang, 2013).

Step-IV: Synthesis of 3-chloro-2-oxo-N-(arylcarbamoyl)-2H-1-benzopyran-6-sulfonamide derivatives
The solid diphosgene (0.40mol) was dissolved in 50 ml chloroform. In another beaker, the corresponding substituted aniline (0.20 mol) was dissolved in 10 ml of chloroform and this was dripped into solid diphosgene solution with ice bath cooling. The reaction mixture was kept for at least 1 h at room temperature and heated with reflux for 6 h, then the corresponding products was obtained by distillation. The 3-chloro-2-oxo-2H-1-benzopyran-6-sulfonamide (3.01 mmo1) was mixed with 20 ml acetone and potassium carbonate (7.2 mmo1) was added to it. This reaction mixture was added to the above reaction mixture and then the reaction mixture was heated with reflux for 1 h. After cooling, the obtained product was filtered, then the filter cake was dissolved with 20 ml water. The solid was obtained by adjusting pH at 1 with concentrated hydrochloric acid and then the solution was neutral by filtering and washing with water(Pingaew et al., 2018). The completion of reaction was monitored by using TLC. The structures of synthesized compounds are illustrated in Fig. 3.

1f [*N-[N-[(2-bromophenyl)carbamoyl]-3-chloro-2-oxo-2H-1-benzopyran-6-sulfonamide*] Pale yellow solid, yield: 76%, molecular formula: $C_{16}H_{10}BrClN_2O_5S$, melting point: 127-129 ^{0}C. Elemental analysis (*cal.*): C, 41.99; H, 2.20; Br, 17.46; Cl, 7.75; N, 6.12; O, 17.48; S, 7.01. FT-IR (neat, cm^{-1}) ν_{max}: 3497 (NH stretch), 3121 (NH bend w), 2987 (Ar stretch), 1751 (C=O stretch), 765 (C=O bend). ^{1}H NMR (300 MHz, DMSO-d_6, chemical shift (ppm)); δ 6.00 (d, NH urea), 7.010, 7.023, 7.039, 7.305, 7.338, 7.474, 7.489, 8.090, 8.092, 8.107 (m, Ar-H). MS m/*z*: 456.21, 457.16 (m+1), 458.09 (m+2), 459.45 (m+3).

1g [*N-[N-[(3-bromophenyl)carbamoyl]-3-chloro-2-oxo-2H-1-benzopyran-6-sulfonamide* Pale yellow solid, yield: 87%, molecular formula: $C_{16}H_{10}BrClN_2O_5S$, melting point: 135-137 ^{0}C. Elemental analysis (*cal.*): C, 41.99; H, 2.20; Br, 17.46; Cl, 7.75; N, 6.12; O, 17.48; S, 7.01. FT-IR (neat, cm^{-1}) ν_{max}: 3462 (NH stretch), 3128 (NH bend w), 2975 (Ar stretch), 1740 (C=O stretch), 763 (C=O bend). ^{1}H NMR (300 MHz, DMSO-d_6, chemical shift (ppm)); δ 6.127 (d, NH urea), 7.020, 7.031, 7.212, 7.335, 7.421, 7.489, 7.491, 8.102, 8.182, 8.201 (m, Ar-H). MS m/*z*: 456.18, 457.20 (m+1), 458.73 (m+2), 460.41 (m+3).

1i [*3-chloro-N-[(2-chlorophenyl)carbamoyl]-2-oxo-2H-1-benzopyran-6-sulfonamide*] Pale yellow semi-solid, yield: 72%, molecular formula: $C_{16}H_{10}Cl_2N_2O_5S$, melting point: 143-145 ^{0}C. Elemental analysis (*cal.*): C, 46.50; H, 2.44; Cl, 17.16; N, 6.78; O, 19.36; S, 7.76. FT-IR (neat, cm^{-1}) ν_{max}: 3465 (NH stretch), 3122 (NH bend w), 2964 (Ar stretch), 1745 (C=O stretch), 768 (C=O bend). ^{1}H NMR (300 MHz, DMSO-d_6, chemical shift (ppm)); δ 6.017 (d, NH urea), 7.010, 7.032, 7.221, 7.329, 7.481, 7.491, 7.498, 8.112, 8.152, 8.210 (m, Ar-H). MS m/*z*: 410.21, 413.16 (m+1), 414.09 (m+2), 416.45 (m+3).

1j [*3-chloro-N-[(3-chlorophenyl)carbamoyl]-2-oxo-2H-1-benzopyran-6-sulfonamide*] Pale yellow semi-solid, yield: 69%, molecular formula: $C_{16}H_{10}Cl_2N_2O_5S$, melting point: 142-144 ^{0}C. Elemental analysis (*cal.*): C, 46.50; H, 2.44; Cl, 17.16; N, 6.78; O, 19.36; S, 7.76. FT-IR (neat, cm^{-1}) ν_{max}: 3470 (NH stretch), 3126 (NH bend w), 2962 (Ar stretch), 1749 (C=O stretch), 762 (C=O bend). ^{1}H NMR (300 MHz, DMSO-d_6, chemical shift (ppm)); δ 6.012 (d, NH urea), 7.123, 7.135, 7.231, 7.332, 7.491, 7.498, 7.521, 8.152, 8.161, 8.281 (m, Ar-H). MS m/*z*: 410.22, 413.19 (m+1), 414.29 (m+2), 416.78 (m+3).

1v [*3-chloro-N-[(2-methylphenyl)carbamoyl]-2-oxo-2H-1-benzopyran-6-sulfonamide*] Pale yellow solid, yield: 74%, molecular formula: $C_{17}H_{13}ClN_2O_5S$, melting point: 122-124 ^{0}C. Elemental analysis (*cal.*): C, 51.98; H, 3.34; Cl, 9.03; N, 7.13; O, 20.37; S, 8.16. FT-IR (neat, cm^{-1}) ν_{max}: 3461 (NH stretch), 3129 (NH bend w), 2966 (Ar stretch), 1750 (C=O stretch), 768 (C=O bend). ^{1}H NMR (300 MHz, DMSO-d_6, chemical shift (ppm)); δ 6.123 (d, NH urea), 2.361 (t, methyl CH_3), 7.103, 7.115, 7.211, 7.322, 7.461, 7.488, 7.511, 8.142, 8.191, 8.282 (m, Ar-H). MS m/*z*: 391.21, 392.28 (m+1), 393.32 (m+2), 394.21 (m+3).

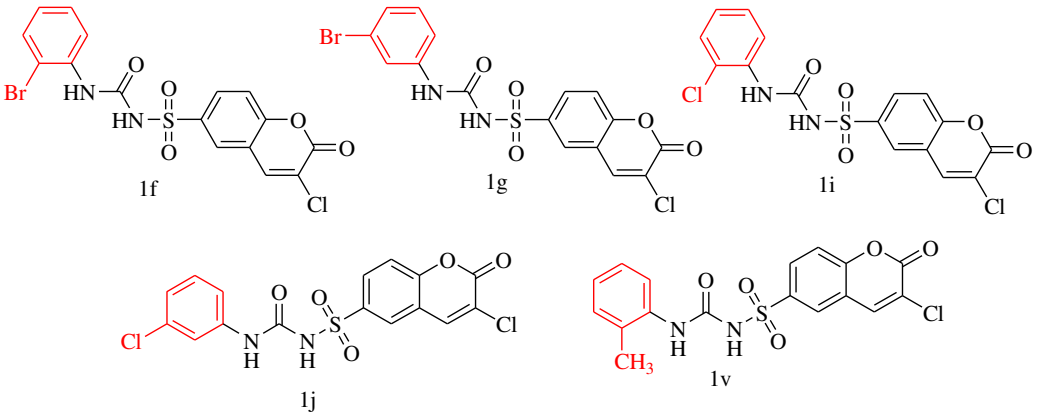

Figure 3. The structures of synthesized compounds

***In vitro* DPP-IV enzyme assay**

Synthesized compounds (**1f, 1g, 1i, 1j, 1v**) were evaluated for inhibition of DPP-IV enzyme by *in vitro* assay. The DPP–IV inhibition assay was performed using assay kit (Cayman chemical kit, Item number: 700210. In a 96-well microtiter plate, the chromogenic substrate was cleared by the serine protease DPP-IV, which resulted in the release of 4-p-nitroaniline (pNA), a yellow-colored product. In brief, the DPP-IV inhibition activities of the compounds at various concentrations were determined by measuring the release of 4pNA from an assay mixture containing 20 µL of DPP-IV enzyme, 0.1 M Tris-HCL buffer (pH 8.0), and varying concentration of the test compounds, with Sitagliptin. After incubation for 10 min, 50 µL of 2 Mm Gly-Pro p-nitroanilide (substrate) was added. The samples were then incubated for 30 min at 37 °C, and the reaction was stopped by the addition of sodium acetate buffer (pH 4.5). The absorbance was measured at 405nm on a microtiter plate reader. Sitagliptin samples was used as standards. A decrease in DPP-IV enzyme activity was observed as the formation of the DNA yellow colored product decreased due to enzyme inhibition. The derivatives were further screened for IC_{50} values in triplicate(Guasch et al., 2012).

Results

Pharmacokinetic features are crucial in drug development because they allow researchers to evaluate the biological elements of potential medications. Lipinski's rule of five and Veber's rules were used to determine if the compounds was ideal for oral bioavailability (Table 1). The coloured zone is the optimum physicochemical region for oral bioavailability, according to the physicochemical radar pictures of the molecules which is given in supplementary file (Table S1). To further understand their pharmacokinetics profiles and drug-likeness properties, all of the proposed compounds were investigated for their ADME characteristics (Table 2).

Table 1
Calculations of Lipinski's rule of five and Veber's rule for the designed derivatives

Compound codes	Lipinski's rule of five					Veber's rule	
	Log P (≤5)	Mol. Wt. (≤500)	HBA (≤10)	HBD (≤5)	Violations	Total polar surface area (Å^2) (≤140)	No. of rotatable bonds (≤10)
Native ligand	3.29	419.37	10	01	00	59.97	03
1a	2.71	378.79	05	02	00	113.86	05
1b	-1.99	470.80	09	04	00	213.18	07
1c	1.11	424.79	07	03	00	163.52	06
1d	1.05	424.79	07	03	00	163.52	06
1e	0.42	424.79	07	03	00	163.52	06
1f	3.20	413.23	05	02	00	113.86	05
1g	3.18	413.23	05	02	00	113.86	05
1h	3.40	413.23	05	02	00	113.86	05
1i	3.20	413.23	05	02	00	113.86	05
1j	3.18	413.23	05	02	00	113.86	05
1k	3.40	413.23	05	02	00	113.86	05
1l	4.20	482.12	05	02	00	113.86	05
1m	3.64	447.68	05	02	00	113.86	05
1n	1.67	459.24	07	03	00	163.52	06
1o	2.12	393.80	05	03	00	125.89	06
1p	2.66	408.81	06	02	00	123.09	06
1q	2.61	408.81	06	02	00	123.09	06
1r	2.51	408.81	06	02	00	123.09	06
1s	2.09	393.80	05	03	00	139.88	05
1t	2.10	393.80	05	03	00	139.88	05
1u	2.14	393.80	05	03	00	139.88	05
1v	2.98	392.81	05	02	00	113.86	05
1w	2.95	392.81	05	02	00	113.86	05
1x	2.92	392.81	05	02	00	113.86	05

Where: Mol. Wt., molecular weight; HBA, hydrogen bond acceptors; HBD, hydrogen bond donors

Table 2
The pharmacokinetics and drug-likeness properties of developed compounds

Compound codes	Pharmacokinetics									Drug-likeness			
	GI abs.	BBB pen.	P-gp sub.	CYP 1A2 inhibitors	CYP 2C19 inhibitors	CYP2 C9 inhibitors	CYP 2D6 inhibitors	CYP 3A4 inhibitors	Log K_p (skin permeation, cm/s)	Ghose	Egan	Muegge	Bioavailability Score
NL	High	Yes	Yes	No	No	No	Yes	No	-7.43	Yes	Yes	Yes	0.55
1a	High	No	No	Yes	No	Yes	No	No	-6.15	Yes	Yes	Yes	0.55
1b	Low	No	Yes	No	No	No	No	No	-7.64	Yes	No	No	0.55

1c	Low	No	No	Yes	Yes	No	No	No	-6.90	Yes	No	No	0.55
1d	Low	No	No	Yes	Yes	No	No	No	-6.90	Yes	No	No	0.55
1e	Low	No	Yes	Yes	Yes	No	No	No	-6.90	Yes	No	No	0.55
1f	High	No	No	Yes	Yes	Yes	No	Yes	-5.94	Yes	Yes	Yes	0.55
1g	High	No	No	Yes	Yes	Yes	No	No	-5.94	Yes	Yes	Yes	0.55
1h	High	No	No	Yes	Yes	Yes	No	Yes	-5.94	Yes	Yes	Yes	0.55
1i	High	No	No	Yes	Yes	Yes	No	Yes	-5.94	Yes	Yes	Yes	0.55
1j	High	No	No	Yes	Yes	Yes	No	No	-5.94	Yes	Yes	Yes	0.55
1k	High	No	No	Yes	Yes	Yes	No	Yes	-5.94	Yes	Yes	Yes	0.55
1l	Low	No	No	Yes	Yes	Yes	No	Yes	-5.47	No	Yes	No	0.55
1m	Low	No	No	Yes	Yes	Yes	No	Yes	-5.70	Yes	Yes	Yes	0.55
1n	Low	No	No	Yes	Yes	No	No	No	-6.67	Yes	No	No	0.55
1o	High	No	No	Yes	No	No	No	No	-6.43	Yes	Yes	Yes	0.55
1p	High	No	No	Yes	No	Yes	No	Yes	-6.38	Yes	Yes	Yes	0.55
1q	High	No	No	Yes	No	Yes	No	Yes	-6.38	Yes	Yes	Yes	0.55
1r	High	No	No	Yes	No	Yes	No	Yes	-6.38	Yes	Yes	Yes	0.55
1s	Low	No	No	Yes	No	Yes	No	No	-6.75	Yes	No	Yes	0.55
1t	Low	No	No	Yes	No	Yes	No	No	-6.75	Yes	No	Yes	0.55
1u	Low	No	No	Yes	No	Yes	No	No	-6.75	Yes	No	Yes	0.55
1v	High	No	No	Yes	Yes	Yes	No	No	-6.00	Yes	Yes	Yes	0.55
1w	High	No	No	Yes	Yes	Yes	No	No	-6.00	Yes	Yes	Yes	0.55
1x	High	No	No	Yes	Yes	Yes	No	No	-6.00	Yes	Yes	Yes	0.55

Where: NL, Native ligand; GI abs., gastrointestinal absorption; BBB pen., blood brain barrier penetration; P-gp sub., p-glycoprotein substrate

From the initial screening through Lipinski rule, Veber's rule, ADME calculations, and drug-likeness properties, molecules 1a, 1f, 1g, 1h, 1i, 1j, 1k, 1o, 1p, 1q, 1r, 1v, 1w, and 1x successfully passed all the filters and displayed most drug-likeness nature. Therefore only these molecules were subjected for molecular docking studies. Many of the molecules selected for docking had exhibited potent interactions and binding energy than native ligand with the target. The active amino acid residues, bond length (A^0), bond type, bond category, binding affinities (kcal/mol), and the ligand energies (kcal/mol) of the docked molecules are tabulated in Table 3. The molecules' 2D and 3D docking postures (most potent) are represented in Fig. 4. The *in vitro* DPP-IV enzyme assay was performed on all of the synthesized compounds and the results are tabulated in Table 4.

Table 3
The active amino acid residues, bond length (A^0), bond type, bond category, binding affinities (kcal/mol), and the ligand energies (kcal/mol)

Active amino residues	Bond length (A^0)	Bond type	Bond category	Ligand energy (kcal/mol)	Binding affinity (kcal/mol)
Native ligand					
TYR662	1.66907	Hydrogen Bond	Conventional Hydrogen Bond	447.3	-9.1
ARG125	4.39768	Electrostatic	Pi-Cation		
ARG358	3.52293				
ARG358	5.41244	Hydrophobic	Pi-Alkyl		
PHE357	3.79334				

1a					
ASN74	2.33789	Hydrogen Bond	Conventional Hydrogen Bond	594.04	-8.4
GLY99	2.35322				
ILE76	5.25362	Hydrophobic	Pi-Alkyl		
1f					
TYR547	2.60818	Hydrogen Bond	Conventional Hydrogen Bond	605.48	-9.3
ARG125	2.49429				
ARG125	1.75026				
TYR752	2.13893				
HIS740	3.57648		Carbon Hydrogen Bond		
ARG125	3.72392	Electrostatic	Pi-Cation		
TRP629	4.10823	Hydrophobic	Pi-Pi Stacked		
TRP629	4.8055				
TRP629	3.80385				
TRP629	4.96247				
TRP627	4.5676		Pi-Alkyl		
TYR662	5.32953				
HIS740	4.31923				
1g					
PRO475	2.90275	Hydrogen Bond	Conventional Hydrogen Bond	606.96	-9
LYS512	2.59036				
ASN562	2.45159				
THR565	2.59155				
ILE529	3.2159	Hydrophobic	Pi-Sigma		
PHE559	5.22399	Other	Pi-Sulfur		
PHE559	5.27503	Hydrophobic	Pi-Pi T-shaped		
ARG560	3.54544		Alkyl		
PRO510	5.48216		Pi-Alkyl		
LYS512	4.63842				
ILE529	4.91916				
LYS512	4.88951				
ARG560	4.44315				
LEU504	5.43192				
MET509	4.92678				
1h					
ARG358	2.28788	Hydrogen Bond	Conventional Hydrogen Bond	611.76	-8.8
TYR547	5.52575	Other	Pi-Sulfur		
PHE357	3.93861	Hydrophobic	Pi-Pi Stacked		
PHE357	4.1694				
1i					
PRO475	2.19185	Hydrogen Bond	Conventional Hydrogen Bond	625.4	-9.1
LYS512	2.4743				
ILE529	3.37388	Hydrophobic	Pi-Sigma		
PHE559	5.51356	Other	Pi-Sulfur		
PHE559	5.1818	Hydrophobic	Pi-Pi T-shaped		

SER511; LYS512	4.82008		Amide-Pi Stacked		
ILE529	4.75793		Alkyl		
ARG560	3.67263				
PRO510	5.3021		Pi-Alkyl		
LYS512	4.66962				
ILE529	5.23664				
LYS512	5.04711				
ARG560	5.0549				
LEU477	5.32189				
1j					
ASN562	2.83589	Hydrogen Bond	Conventional Hydrogen Bond	609.81	-9.1
THR565	2.57034				
ARG560	2.95933		Pi-Donor Hydrogen Bond		
ILE529	3.41743	Hydrophobic	Pi-Sigma		
PHE559	5.47334	Other	Pi-Sulfur		
PHE559	5.09281	Hydrophobic	Pi-Pi T-shaped		
LYS512	5.23401		Alkyl		
ILE529	5.45064				
ARG560	3.4898				
PRO475	4.97756				
LEU514	3.73636				
PRO510	5.29506		Pi-Alkyl		
LYS512	4.77415				
ILE529	5.29563				
LYS512	4.66648				
ARG560	4.70736				
PRO475	4.03594				
1k					
ARG358	2.34123	Hydrogen Bond	Conventional Hydrogen Bond	611.88	-8.8
GLN553	2.78523		Pi-Donor Hydrogen Bond		
TYR547	5.57297	Other	Pi-Sulfur		
PHE357	4.14429	Hydrophobic	Pi-Pi Stacked		
PHE357	4.2369				
1o					
ARG358	2.29775	Hydrogen Bond	Conventional Hydrogen Bond	602.53	-9
TYR547	2.04649				
GLN553	2.76723		Pi-Donor Hydrogen Bond		
TYR547	3.99447	Hydrophobic	Pi-Sigma		
TYR547	5.54888	Other	Pi-Sulfur		
PHE357	4.02628	Hydrophobic	Pi-Pi Stacked		
PHE357	4.19639				
1p					

ARG358	2.29775	Hydrogen Bond	Conventional Hydrogen Bond	622.45	-8.5
TYR547	2.04649				
GLN553	2.76723		Pi-Donor Hydrogen Bond		
TYR547	3.99447	Hydrophobic	Pi-Sigma		
TYR547	5.54888	Other	Pi-Sulfur		
PHE357	4.02628	Hydrophobic	Pi-Pi Stacked		
PHE357	4.19639				
1q					
ARG358	2.21993	Hydrogen Bond	Conventional Hydrogen Bond	626.99	-8.6
TYR547	2.13277				
ARG358	3.76053		Carbon Hydrogen Bond		
GLN553	2.81214		Pi-Donor Hydrogen Bond		
TYR547	5.61595	Other	Pi-Sulfur		
PHE357	3.97274	Hydrophobic	Pi-Pi Stacked		
PHE357	4.21343				
1r					
ARG358	2.28539	Hydrogen Bond	Conventional Hydrogen Bond	627.77	-8.7
ARG358	3.77937		Carbon Hydrogen Bond		
GLN553	2.78115		Pi-Donor Hydrogen Bond		
TYR547	5.57326	Other	Pi-Sulfur		
PHE357	4.02059	Hydrophobic	Pi-Pi Stacked		
PHE357	4.2177				
1v					
PRO475	2.49944	Hydrogen Bond	Conventional Hydrogen Bond	626.1	-9
LYS512	2.63104				
ASN562	2.5893				
THR565	2.62445				
ILE529	3.23525	Hydrophobic	Pi-Sigma		
PHE559	5.27245	Other	Pi-Sulfur		
PHE559	5.20996	Hydrophobic	Pi-Pi T-shaped		
ILE529	5.49304		Alkyl		
ARG560	3.53527				
LEU477	4.0075				
LEU504	4.76275				
LYS512	4.56438		Pi-Alkyl		
ILE529	5.03503				
LYS512	4.79616				
ARG560	4.48863				
PHE559	4.67305				
1w					
ARG358	2.25345	Hydrogen	Conventional	621.76	-8.6

		Bond	Hydrogen Bond		
ARG358	3.68677		Carbon Hydrogen Bond		
GLN553	2.88096		Pi-Donor Hydrogen Bond		
TYR547	5.65234	Other	Pi-Sulfur		
PHE357	4.04205	Hydrophobic	Pi-Pi Stacked		
PHE357	4.20358				
TYR585	4.8959		Pi-Alkyl		
1x					
ARG358	2.33701	Hydrogen Bond	Conventional Hydrogen Bond	611.72	-8.9
TYR547	2.09119				
TYR547	5.62126	Other	Pi-Sulfur		
PHE357	4.20082	Hydrophobic	Pi-Pi Stacked		
PHE357	4.32083				

3D-docking poses

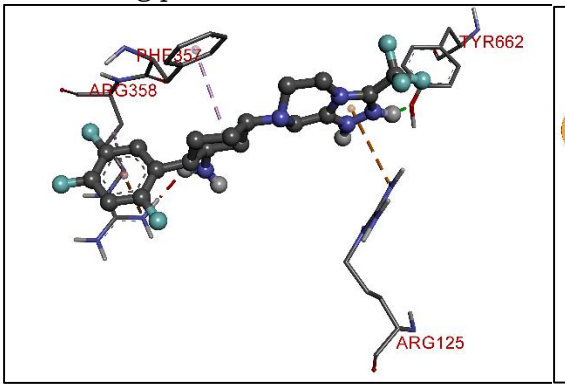

2D-docking poses

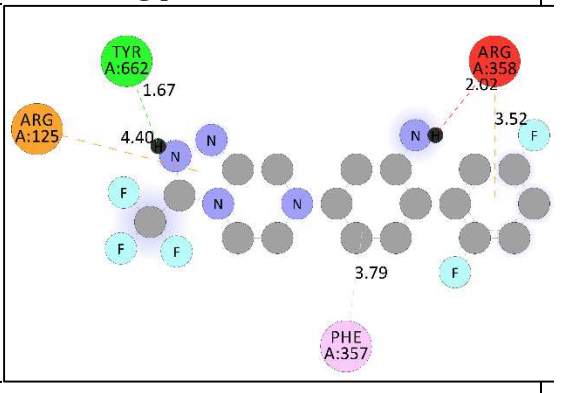

Native ligand

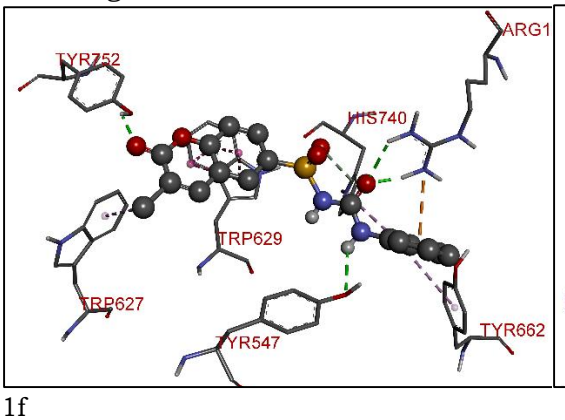

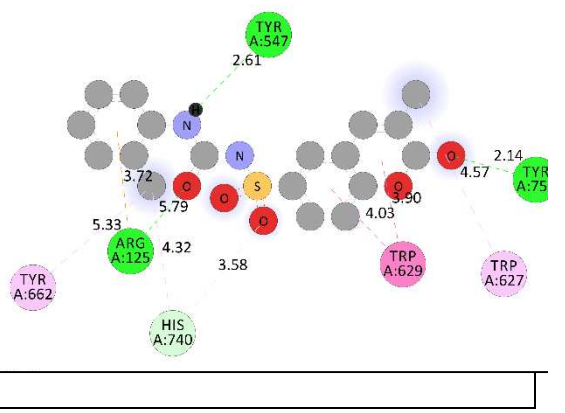

1f

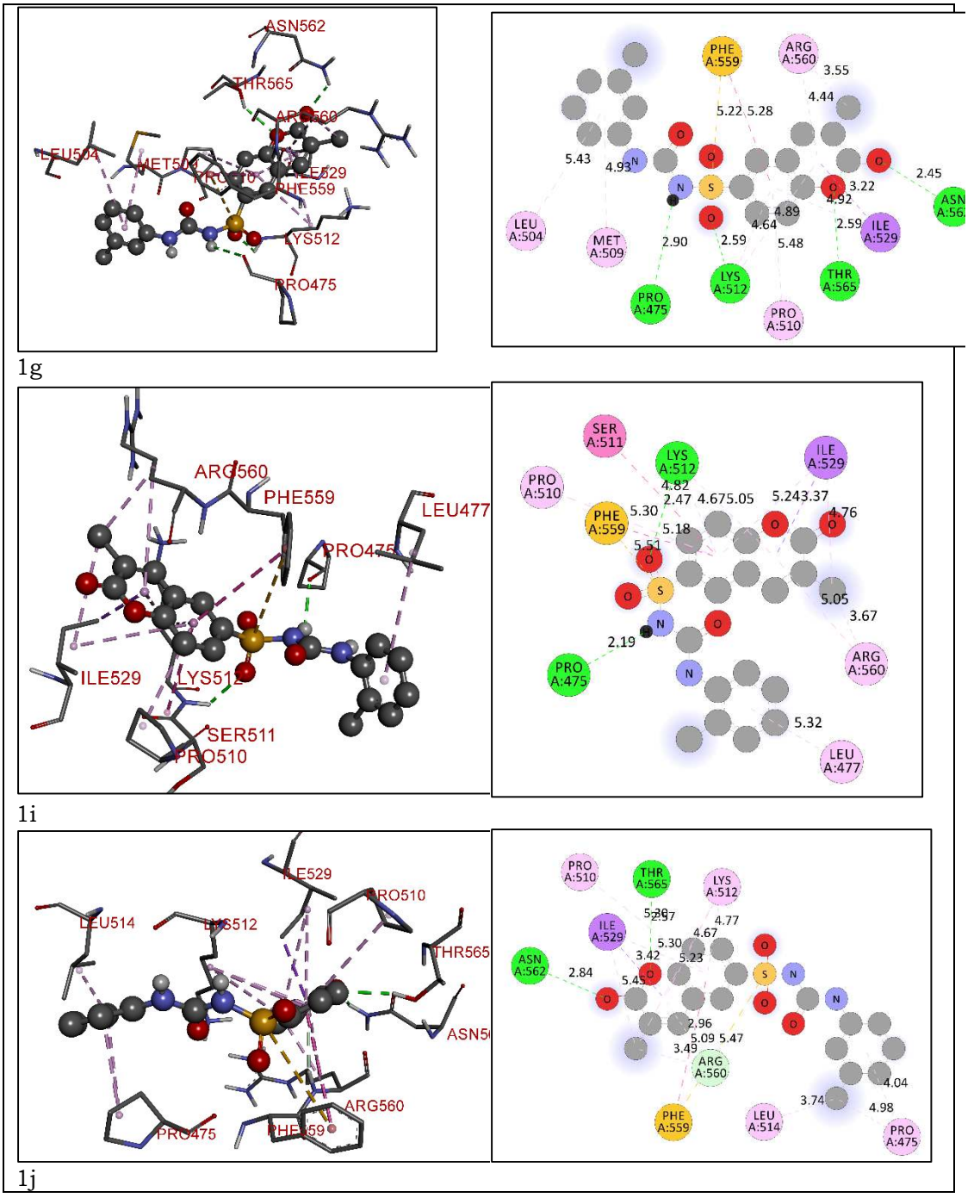
ASN562
THR565
ARG560
LEU504
MET509
PRO510
ILE529
PHE559
LYS512
PRO475
PHE A:559
ARG A:560
LEU A:504
MET A:509
LYS A:512
THR A:565
PRO A:475
PRO A:510
ILE A:529
1g
ARG560
PHE559
LEU477
PRO475
ILE529
LYS512
SER511
PRO510
SER A:511
LYS A:512
ILE A:529
PRO A:510
PHE A:559
ARG A:560
PRO A:475
LEU A:477
1i
ILE529
PRO510
LEU514
LYS512
THR565
ARG560
PRO475
PHE559
PRO A:510
THR A:565
LYS A:512
ILE A:529
ASN A:562
ARG A:560
PHE A:559
LEU A:514
PRO A:475
1j

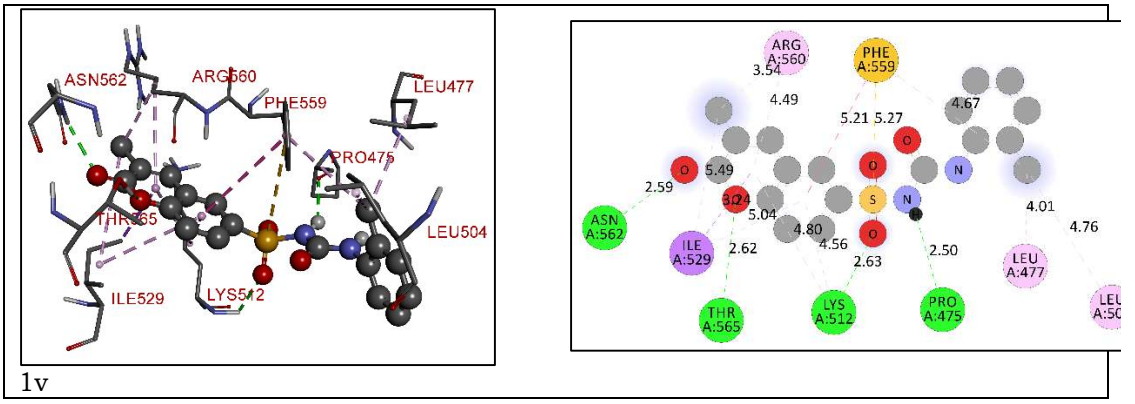

1v

Figure 4. The binding poses and 2D interactions of native ligand, and most potent derivatives

Table 4
In vitro DPP-IV enzyme assay of synthesized compounds

Compound code	% Inhibition at 250 and 50 µM	IC_{50} (µM) (Prism software)
Sitagliptin (100 µM)	102.6	0.018
1f	95.5	15.55
1g	92.1	15.85
1i	91.4	13.95
1j	94.5	14.48
1v	86.1	13.45

Discussion

It is the primary goal of medication development to transform a therapeutic molecule into a dosage form that can be administered to patients. Pharmacological effects must occur at the site of action and be eradicated within an acceptable time period; this is preferable to once-a-day use. It is possible to make risk-based evaluations of a novel drug's safety by characterizing its absorption, distribution, metabolism, and excretion (ADME) features(Akhtar et al., 2017; Barret, 2018; Kamal et al., 2015). This helps to study and explain how pharmacokinetic processes occur. We have designed some 3-chloro-2-oxo-N-(arylcarbamoyl)-2H-1-benzopyran-6-sulfonamides as potential DPP-IV inhibitors through rational drug design approach. All the designed derivatives were subjected for ADME analysis.

In accordance with Lipinski's and Veber's rule (Table 1), none of the molecule has violated the Lipinski rule of five but few has violated the Veber's rule. The log P values of all the molecules found between -1.99 to 4.20 which indicate optimum lipophilicity. Lipophilicity is a significant feature of the molecule that affects how it works in the body(S. Khan et al., 2021). It is determined by the compound's Log P value, which measures the drug's permeability in the body to reach the target tissue(Krzywinski and Altman, 2013; Lipinski et al., 2012). The molecular weight of all the molecules was below 500 Da which indicates active better transport of

the molecules through biological membrane. Fortunately, the Lipinski rule of 5 had not been compromised by the compounds, including native ligand (Khan et al., 2022; Shntaif et al., 2021). The total polar surface area (TPSA) and the number of rotatable bonds has been found to better discriminate between compounds that are orally active or not. According to Veber's rule, TPSA should be ≤ 140 and number of rotatable bonds should be ≤ 10. It was observed that compounds **1b, 1c, 1d, 1e,** and **1n** violated the Veber's rule, as it has TPSA more than 140Å^2 which indicate its poor oral bioavailability.

In order to further optimize the compounds, pharmacokinetics and drug-likeness properties were calculated for each one. All the compounds excluding native ligand showed no penetration to the blood-brain barrier (BBB). The log *Kp* (skin penetration, cm/s) and bioavailability values of all the compounds were within acceptable limits. Few molecules do not meet all, two, or one of the Ghose, Egan, and Muegge requirements (Table 2). Many molecules found to be cytochrome enzyme inhibitors which indicates they will might be interfere with metabolism of other drugs. Molecules **1b, 1c, 1d, 1e, 1l, 1m, 1n, 1s, 1t,** and **1u** exhibited low gastrointestinal (GI) absorption therefore these molecules were eliminated from further screening and did not subjected for molecular docking studies.

The binding affinities of all the docked derivatives have been compared with the binding mode of native ligand present in the crystal structure of DPP-IV enzyme (PDB ID: 2P8S). Native ligand exhibited -9.1 kcal/mol binding affinity with enzyme and formed only one conventional hydrogen bond with Ty662. It has developed two electrostatic (Pi-cation) bonds with Arg125 and Arg358. It has exhibited hydrophobic (Pi-alkyl) bonds with Arg358 and Phe357. Compound **1f** displayed -9.3 kcal/mol binding affinity and formed four conventional hydrogen bonds with Tyr547, Arg125, Tyr752 and one carbon-hydrogen bond with His740. It has formed only one electrostatic bond with Arg125 and many hydrophobic bonds with Trp629, Trp627, Tyr662, and His740. Compound **1g** showed -9 kcal/mol binding affinity and formed four conventional hydrogen bonds with Pro475, Lys512, Asn562, and Thr565. It has developed many hydrophobic bonds with Ile529, Phe559, Arg560, Pro510, Lys512, Ile529, Arg560, Leu504, and Met509. Compound **1i** exhibited -9.1 kcal/mol docking score and formed two conventional hydrogen bonds with Pro475 and Lys512. It has developed many hydrophobic interactions (Pi-sigma, Pi-sulfur, Pi-Pi T-shaped, Amide-Pi-stacked, alkyl, and Pi-alkyl) with Ile529, Phe559, Ser511, Lys512, Arg560, Pro510, and Leu477. Compound **1j** formed two conventional hydrogen bond with Asn562, Thr565 and one Pi-donor hydrogen bond with Arg560 and exhibited -9.1 kcal/mol. It has developed many hydrophobic interactions in same as compound 1i displayed. Compound **1v** exhibited -9 kcal/mol docking score and it has demonstrated interactions in a same way as compound **1i** and **1j** developed. Therefore from this investigation we have selected **1f, 1g, 1i, 1j,** and **1v** for the wet lab synthesis and biological evaluation. The structures of all the synthesized compounds were confirmed by spectral analysis and were subjected for *in vitro* DPP-IV enzyme assay. Sitagliptin was used as standard for the assay and it displayed 0.018 μM IC_{50} value. Compound **1f, 1g, 1i, 1j,** and **1v** exhibited 15.55, 15.85, 13.95, 14.48, and 13.45 μM IC_{50} values respectively.

Conclusion

DPP-IV inhibitors are the agents that gained extensive interest in T2DM treatment with proved long term efficacy and better glycemic control. In present work, we aimed at preparing coumarin and sulfonamide containing moieties into a single candidate template i.e. 3-chloro-2-oxo-N-(arylcarbamoyl)-2H-1-benzopyran-6-sulfonamides for the purpose of synergistic activity. The designed derivatives were subjected for the calculations of Lipinski rule, Veber's rule, ADME analysis, drug-likeness properties and molecular docking. The derivatives which successfully passed all the criteria were proceeded for wet lab synthesis and biological evaluation. We concluded that compound **1f, 1g, 1i, 1j,** and **1v** are potential lead compounds to be developed as potent DPP-IV inhibitors for the treatment of diabetes. Many more clinical data needs to be generated using numerous *in vitro* and *in vivo* models to prove their therapeutics effectiveness as DPP-IV inhibitors.

References

Akhtar, W., Khan, M.F., Verma, G., Shaquiquzzaman, M., Rizvi, M.A., Mehdi, S.H., Akhter, M., Alam, M.M., 2017. Therapeutic evolution of benzimidazole derivatives in the last quinquennial period. Eur. J. Med. Chem. 126, 705–753. https://doi.org/10.1016/j.ejmech.2016.12.010

Artasensi, A., Pedretti, A., Vistoli, G., Fumagalli, L., 2020. Type 2 diabetes mellitus: A review of multi-target drugs. Molecules 25. https://doi.org/10.3390/molecules25081987

Arulmozhi, D.K., Portha, B., 2006. GLP-1 based therapy for type 2 diabetes. Eur. J. Pharm. Sci. 28, 96–108. https://doi.org/10.1016/j.ejps.2006.01.003

Barret, R., 2018. Lipinski's Rule of Five, in: Therapeutical Chemistry. pp. 97–100. https://doi.org/10.1016/b978-1-78548-288-5.50006-8

Basanagouda, M., Shivashankar, K., Kulkarni, M. V., Rasal, V.P., Patel, H., Mutha, S.S., Mohite, A.A., 2010. Synthesis and antimicrobial studies on novel sulfonamides containing 4-azidomethyl coumarin. Eur. J. Med. Chem. 45, 1151–1157. https://doi.org/10.1016/j.ejmech.2009.12.022

Chaudhari, R.N., Khan, S.L., Chaudhary, R.S., Jain, S.P., Siddiqui, F.A., 2020. B-Sitosterol: Isolation from Muntingia Calabura Linn Bark Extract, Structural Elucidation And Molecular Docking Studies As Potential Inhibitor of SARS-CoV-2 Mpro (COVID-19). Asian J. Pharm. Clin. Res. 13, 204–209. https://doi.org/10.22159/ajpcr.2020.v13i5.37909

Daina, A., Michielin, O., Zoete, V., 2017. SwissADME: A free web tool to evaluate pharmacokinetics, drug-likeness and medicinal chemistry friendliness of small molecules. Sci. Rep. 7. https://doi.org/10.1038/srep42717

Dallakyan, S., Olson, A.J., 2015. Small-molecule library screening by docking with PyRx. Methods Mol. Biol. 1263, 243–250. https://doi.org/10.1007/978-1-4939-2269-7_19

De Souza, S.M., Delle Monache, F., Smânia, A., 2005. Antibacterial activity of coumarins. Zeitschrift fur Naturforsch. - Sect. C J. Biosci. 60, 693–700. https://doi.org/10.1515/znc-2005-9-1006

Dowarah, J., Singh, V.P., 2020. Anti-diabetic drugs recent approaches and advancements. Bioorganic Med. Chem. 28. https://doi.org/10.1016/j.bmc.2019.115263

Galayev, O., Garazd, Y., Garazd, M., Lesyk, R., 2015. Synthesis and anticancer activity of 6-heteroarylcoumarins. Eur. J. Med. Chem. 105, 171–181. https://doi.org/10.1016/j.ejmech.2015.10.021

Galicia-Garcia, U., Benito-Vicente, A., Jebari, S., Larrea-Sebal, A., Siddiqi, H., Uribe, K.B., Ostolaza, H., Martín, C., 2020. Pathophysiology of type 2 diabetes mellitus. Int. J. Mol. Sci. 21, 1–34. https://doi.org/10.3390/ijms21176275

Grewal, A.S., Lather, V., Charaya, N., Sharma, N., Singh, S., Kairys, V., 2020. Recent Developments in Medicinal Chemistry of Allosteric Activators of Human Glucokinase for Type 2 Diabetes Mellitus Therapeutics. Curr. Pharm. Des. 26, 2510–2552. https://doi.org/10.2174/1381612826666200414163148

Guasch, L., Ojeda, M.J., González-Abuín, N., Sala, E., Cereto-Massagué, A., Mulero, M., Valls, C., Pinent, M., Ardévol, A., Garcia-Vallvé, S., Pujadas, G., 2012. Identification of Novel Human Dipeptidyl Peptidase-IV Inhibitors of Natural Origin (Part I): Virtual Screening and Activity Assays. PLoS One 7. https://doi.org/10.1371/journal.pone.0044971

Huang, J., Deng, X., Zhou, S., Wang, N., Qin, Y., Meng, L., Li, G., Xiong, Y., Fan, Y., Guo, L., Lan, D., Xing, J., Jiang, W., Li, Q., 2019. Identification of novel uracil derivatives incorporating benzoic acid moieties as highly potent Dipeptidyl Peptidase-IV inhibitors. Bioorganic Med. Chem. 27, 644–654. https://doi.org/10.1016/j.bmc.2019.01.001

Kamal, A., Shaik, A.B., Jain, N., Kishor, C., Nagabhushana, A., Supriya, B., Bharath Kumar, G., Chourasiya, S.S., Suresh, Y., Mishra, R.K., Addlagatta, A., 2015. Design and synthesis of pyrazole-oxindole conjugates targeting tubulin polymerization as new anticancer agents. Eur. J. Med. Chem. 92, 501–513. https://doi.org/10.1016/j.ejmech.2013.10.077

Kelly, S.D., Neary, S.L., 2020. Ominous Octet and Other Scary Diabetes Stories: The Overview of Pathophysiology of Type 2 Diabetes Mellitus. Physician Assist. Clin. 5, 121–133. https://doi.org/10.1016/j.cpha.2019.11.002

Khan, A., Unnisa, A., Sohel, M., Date, M., Panpaliya, N., Saboo, S.G., Siddiqui, F., Khan, S., 2022. Investigation of phytoconstituents of Enicostemma littorale as potential glucokinase activators through molecular docking for the treatment of type 2 diabetes mellitus. Silico Pharmacol. 10. https://doi.org/10.1007/s40203-021-00116-8

Khan, S., Kale, M., Siddiqui, F., Nema, N., 2021. Novel pyrimidine-benzimidazole hybrids with antibacterial and antifungal properties and potential inhibition of SARS-CoV-2 main protease and spike glycoprotein. Digit. Chinese Med. 4, 102–119. https://doi.org/10.1016/j.dcmed.2021.06.004

Khan, S.L., Siddiqui, F.A., Shaikh, M.S., Nema, N. V., Shaikh, A.A., 2021. Discovery of potential inhibitors of the receptor-binding domain (RBD) of pandemic disease-causing SARS-CoV-2 Spike Glycoprotein from Triphala through molecular docking. Curr. Chinese Chem. 01. https://doi.org/10.2174/2666001601666210322121802

Khan, S.L., Sonwane, G.M., Siddiqui, F.A., Jain, S.P., Kale, M.A., Borkar, V.S., 2020. Discovery of Naturally Occurring Flavonoids as Human Cytochrome P450 (CYP3A4) Inhibitors with the Aid of Computational Chemistry. Indo Glob. J. Pharm. Sci. 10, 58–69. https://doi.org/10.35652/igjps.2020.10409

Khan, Sharuk L; Siddiui, F.A., 2020. Beta-Sitosterol: As Immunostimulant, Antioxidant and Inhibitor of SARS-CoV-2 Spike Glycoprotein. Arch. Pharmacol. Ther. 2. https://doi.org/10.33696/pharmacol.2.014

Kim, S., Chen, J., Cheng, T., Gindulyte, A., He, J., He, S., Li, Q., Shoemaker, B.A., Thiessen, P.A., Yu, B., Zaslavsky, L., Zhang, J., Bolton, E.E., 2021. PubChem in 2021: New data content and improved web interfaces. Nucleic Acids Res. 49, D1388–D1395. https://doi.org/10.1093/nar/gkaa971

Krzywinski, M., Altman, N., 2013. Points of significance: Significance, P values and t-tests. Nat. Methods 10, 1041–1042. https://doi.org/10.1038/nmeth.2698

Lipinski, C.A., Lombardo, F., Dominy, B.W., Feeney, P.J., 2012. Experimental and computational approaches to estimate solubility and permeability in drug discovery and development settings. Adv. Drug Deliv. Rev. https://doi.org/10.1016/j.addr.2012.09.019

Mali, R.S., Deshpande, J. V., 1995. Facile synthesis of 3-chlorocoumarins. Org. Prep. Proced. Int. 27, 663–667. https://doi.org/10.1080/00304949509458527

Miyata, T., 2015. Discovery studio modeling environment. Ensemble 17, 98–104.

Molinspiration cheminformatics, 2006. . Choice Rev. Online 43, 43-6538-43–6538. https://doi.org/10.5860/choice.43-6538

Okechukwu, P., Sharma, M., Tan, W.H., Chan, H.K., Chirara, K., Gaurav, A., Al-Nema, M., 2020. In-vitro anti-diabetic activity and in-silico studies of binding energies of palmatine with alpha-amylase, alpha-glucosidase and DPP-IV enzymes. Pharmacia 67, 363–371. https://doi.org/10.3897/pharmacia.67.e58392

Pingaew, R., Mandi, P., Prachayasittikul, Veda, Prachayasittikul, S., Ruchirawat, S., Prachayasittikul, Virapong, 2018. Synthesis, molecular docking, and QSAR study of sulfonamide-based indoles as aromatase inhibitors. Eur. J. Med. Chem. 143, 1604–1615. https://doi.org/10.1016/j.ejmech.2017.10.057

Qi, G., Zhang, W., 2013. Synthesis of new coumarin compounds and its hypoglycemic activity and structure-activity relationship. Asian J. Chem. 25, 9835–9839. https://doi.org/10.14233/ajchem.2013.15453

Rappé, A.K., Casewit, C.J., Colwell, K.S., Goddard, W.A., Skiff, W.M., 1992. UFF, a Full Periodic Table Force Field for Molecular Mechanics and Molecular Dynamics Simulations. J. Am. Chem. Soc. 114, 10024–10035. https://doi.org/10.1021/ja00051a040

Safavi, M., Foroumadi, A., Abdollahi, M., 2013. The importance of synthetic drugs for type 2 diabetes drug discovery. Expert Opin. Drug Discov. 8, 1339–1363. https://doi.org/10.1517/17460441.2013.837883

Salvatore, T., Carbonara, O., Cozzolino, D., Torella, R., Carlo Sasso, F., 2007. Adapting the GLP-1-Signaling System to the Treatment of Type 2 Diabetes. Curr. Diabetes Rev. 3, 15–23. https://doi.org/10.2174/157339907779802076

Sashidhara, K. V., Rao, K.B., Singh, S., Modukuri, R.K., Aruna Teja, G., Chandasana, H., Shukla, S., Bhatta, R.S., 2014. Synthesis and evaluation of new 3-phenylcoumarin derivatives as potential antidepressant agents. Bioorganic Med. Chem. Lett. 24, 4876–4880. https://doi.org/10.1016/j.bmcl.2014.08.037

Shntaif, A.H., Khan, S., Tapadiya, G., Chettupalli, A., Saboo, S., Shaikh, M.S., Siddiqui, F., Amara, R.R., 2021. Rational drug design, synthesis, and biological evaluation of novel N-(2-arylaminophenyl)-2,3-diphenylquinoxaline-6-sulfonamides as potential antimalarial, antifungal, and antibacterial agents. Digit. Chinese Med. 4, 290–304. https://doi.org/10.1016/j.dcmed.2021.12.004

Siddiqui, F.A., Khan, S.L., Marathe, R.P., Nema, N. V., 2021. Design, Synthesis, and In Silico Studies of Novel N-(2-Aminophenyl)-2,3- Diphenylquinoxaline-6-Sulfonamide Derivatives Targeting Receptor- Binding Domain (RBD) of SARS-CoV-2 Spike Glycoprotein and their Evaluation as Antimicrobial and Antimalarial Agents. Lett. Drug Des. Discov. 18, 915–931. https://doi.org/10.2174/1570180818666210427095203

Simos, Y. V., Spyrou, K., Patila, M., Karouta, N., Stamatis, H., Gournis, D., Dounousi, E., Peschos, D., 2020. Trends of nanotechnology in type 2 diabetes mellitus treatment. Asian J. Pharm. Sci. https://doi.org/10.1016/j.ajps.2020.05.001

Stoimenis, D., Karagiannis, T., Katsoula, A., Athanasiadou, E., Kazakos, K., Bekiari, E., Matthews, D.R., Tsapas, A., 2017. Once-weekly dipeptidyl peptidase-4 inhibitors for type 2 diabetes: a systematic review and meta-analysis. Expert Opin. Pharmacother. 18, 843–851. https://doi.org/10.1080/14656566.2017.1324848

Tamene, D., Endale, M., 2019. Antibacterial Activity of Coumarins and Carbazole Alkaloid from Roots of Clausena anisata. Adv. Pharmacol. Sci. 2019. https://doi.org/10.1155/2019/5419854

Teoh, S.L., Das, S., 2018. Phytochemicals and their effective role in the treatment of diabetes mellitus: a short review. Phytochem. Rev. 17, 1111–1128. https://doi.org/10.1007/s11101-018-9575-z

Vojislav, C., Natasa, R., Milica, P., Slobodan, A., Radivoj, K., Danijela, R., Sasa, R., 2020. Incidence trend of type 1 diabetes mellitus in Serbia. BMC Endocr. Disord. 20. https://doi.org/10.1186/s12902-020-0504-y